Resting-State Functional Connectivity Predicts Cochlear-Implant Speech Outcomes

Jamal Esmaelpoor,[1,2] Tommy Peng,[1,2] Beth Jelfs,[3] Darren Mao,[1,2] Maureen J. Shader,[4] and Colette M. McKay[1,2]

Objectives: Cochlear implants (CIs) have revolutionized hearing restoration for individuals with severe or profound hearing loss. However, a substantial and unexplained variability persists in CI outcomes, even when considering subject-specific factors such as age and the duration of deafness. In a pioneering study, we use resting-state functional near-infrared spectroscopy to predict speech-understanding outcomes before and after CI implantation. Our hypothesis centers on resting-state functional connectivity (FC) reflecting brain plasticity post-hearing loss and implantation, specifically targeting the average clustering coefficient in resting FC networks to capture variation among CI users.

Design: Twenty-three CI candidates participated in this study. Resting-state functional near-infrared spectroscopy data were collected pre-implantation and at 1 month, 3 months, and 1 year postimplantation. Speech understanding performance was assessed using consonant-nucleus-consonant words in quiet and Bamford-Kowal-Bench sentences in noise 1-year postimplantation. Resting-state FC networks were constructed using regularized partial correlation, and the average clustering coefficient was measured in the signed weighted networks as a predictive measure for implantation outcomes.

Results: Our findings demonstrate a significant correlation between the average clustering coefficient in resting-state functional networks and speech understanding outcomes, both pre- and postimplantation.

Conclusions: This approach uses an easily deployable resting-state functional brain imaging metric to predict speech-understanding outcomes in implant recipients. The results indicate that the average clustering coefficient, both pre- and postimplantation, correlates with speech understanding outcomes.

Key words: Clustering coefficient, Cochlear implants, fNIRS, Outcome prediction, Resting-state functional connectivity.

(Ear & Hearing 2024;XX;00–00)

INTRODUCTION

Cochlear implants (CIs) have been instrumental in restoring hearing for individuals with severe to profound hearing loss. However, a significant proportion of CI users experience suboptimal outcomes or limited benefit from the implant (Boisvert et al. 2020). Although case-history factors such as age, duration of deafness, residual hearing, and previous experience with hearing aids have been investigated to explain this variability, they account for only a fraction of the variance in implantation outcomes (Blamey et al. 2012; Lazard et al. 2012; Dunn et al. 2014). As a result, researchers are increasingly seeking more dependable predictors of speech understanding outcomes, particularly by examining changes in central cortical language networks. These networks are thought to be more closely linked to CI performance than the neural responses observed at lower levels of the auditory system, such as the brainstem or auditory nerves (Fallon et al. 2008; Liang et al. 2018; Glennon et al. 2020; Fullerton et al. 2023).

Numerous studies have indicated neuroplastic changes in the brain following hearing loss and cochlear implantation, which can be broadly categorized as cross-modal and adaptive structural changes (Glennon et al. 2020). Sensory deprivation in one modality is known to lead to increased activity in brain regions associated with the remaining senses, resulting in the colonization of the primary cortical area by other modalities (Bavelier & Neville 2002; Merabet & Pascual-Leone 2010). Individuals with severe hearing loss often rely on intact senses, such as vision, to compensate for their hearing impairment. For instance, the auditory cortex in these individuals becomes more receptive to visual stimulation, enabling better visual localization and motion detection (Kral & Sharma 2023). Some researchers argue that these cross-modal changes and the recruitment of the auditory cortex by other modalities may have maladaptive effects following cochlear implantation (Merabet & Pascual-Leone 2010; Sandmann et al. 2012). For example, Doucet et al. (2006) compared evoked potentials in response to visual stimuli of concentric gratings and found broader, anteriorly distributed cortical activations in patients with poorer speech understanding performance. Conversely, other studies suggest that these cross-modal changes in the auditory cortex may actually enhance CI users' performance. They propose that the enhanced cross-modal plasticity in the auditory cortex improves visual speech understanding, leading to better lipreading abilities and speech understanding performance (Strelnikov et al. 2013; Anderson et al. 2017; Fullerton et al. 2023). Anderson et al. (2017) investigated cross-modal activation of the auditory cortex by visual speech before and 6 mo after cochlear implantation, also based on functional near-infrared spectroscopy (fNIRS) recordings. Their findings demonstrated a positive correlation between increased auditory cortex activation and CI recipients' speech understanding ability 6 mo after implantation. However, drawing definitive conclusions on the adaptive or maladaptive

[1]Department of Medical Bionics, University of Melbourne, Melbourne, Australia; [2]The Bionics Institute of Australia, Melbourne, Australia; [3]Department of Electronic, Electrical and Systems Engineering, University of Birmingham, Birmingham, United Kingdom; and [4]Department of Speech, Language, and Hearing Sciences, Purdue University, West Lafayette, Indiana, USA.

Supplemental digital content is available for this article. Direct URL citations appear in the printed text and are provided in the HTML and text of this article on the journal's Web site (www.ear-hearing.com).

<zdoi; 10.1097/AUD.0000000000001564>

effects of cross-modal changes is challenging due to the wide variability in visual and audio stimuli used in these studies. Neuroimaging evidence reveals that different types of speech stimuli elicit distinct brain activation patterns (Peelle 2019), including separate words and syllables, continuous speech for lingual visual and audio stimuli (Calvert et al. 1997; Anderson et al. 2017; Shader et al. 2021) and speech-like noise or checkerboards as nonlingual or visual stimuli (Chen et al. 2016; Fullerton et al. 2023), each potentially leading to different activity patterns in the brain.

In addition to cross-modal changes, hearing loss is associated with significant adaptive structural changes in brain regions supporting auditory, language, and cognitive processing. These changes involve gray matter reduction in the inferior, middle, and superior temporal lobes, as well as the frontal and lingual gyrus. These structural alterations in the brain due to hearing loss affect auditory abilities and are linked to other cognitive dysfunctions, such as deficits in language function and semantic memory (Yang et al. 2014; Jafari et al. 2021; Kim et al. 2021). Furthermore, these structural changes can impact hearing abilities following cochlear implantation (Moore & Shannon 2009; Gordon et al. 2011). Given that the brain's structural connectivity network forms the basis for functional connectivity (FC) (Damoiseaux & Greicius 2009; Carlson et al. 2020; Liégeois et al. 2020), assessing resting-state FC (also known as the intrinsic functional network) provides a means to evaluate these subtle changes in the brain network. Resting-state FC refers to the statistical dependence between activities in different brain regions (nodes in graph theory) in the absence of explicit stimuli or tasks. Investigating various features of resting-state functional networks has become prominent in studying and predicting diverse brain disorders, including consciousness (Yu et al. 2021), Alzheimer (Cecchetti et al. 2021), and depression (Craddock et al. 2009), as well as investigating brain dynamics during learning (Kollndorfer et al. 2015) and aging (Escrichs et al. 2021).

The aim of this study was to pinpoint a reliable indicator of cochlear implantation outcomes for individuals with postlingual deafness, using the resting-state functional networks of the brain. To achieve this objective, we propose that variations in adaptive changes within brain regions associated with the hearing network in these individuals can be reflected by the average clustering coefficient in the resting-state functional network, which quantifies the tendency of neighboring nodes to cluster together in graph theory (Fornito et al. 2016). Given that the brain relies on physical neural connections (Bullmore & Sporns 2012; Kral & Sharma 2023), our hypothesis is based on the assumption that less neural atrophy in the brain is associated with more densely connected nodes in the brain's functional network and better behavioral speech performance. Furthermore, we conducted fNIRS recordings at various time points pre- and postimplantation to assess the plastic changes in the proposed measure resulting from the newly applied brain stimulation provided by the device. We measure FC between pairs of channels using partial correlation (Liégeois et al. 2020). To the best of our knowledge, this is the first study to evaluate resting-state FC for assessing brain plasticity in CI recipients and to propose an indicator of speech understanding outcomes. By concentrating on resting-state FC, our approach offers a streamlined, concise, and straightforward assessment, circumventing the complexities associated with task-based experimental design and result interpretation. In addition, we used fNIRS for brain imaging, a noninvasive and cost-effective optical imaging technology. It is important to note that, the implant device does not interfere with fNIRS measurements (Shader et al. 2021).

MATERIALS AND METHODS

Participants

Twenty-seven adult CI recipients took part in the study. There were no criteria for recruiting CI recipients, except that all participants were postlingually deaf and had been implanted with Nucleus brand devices. However, 4 participants did not complete the final test at 12 months. So, they were excluded from the study, and the results reported here are based on the data acquired from the remaining 23 subjects (mean age = 58.1 ± 19.3, 11 female). Table 1 provides the demographic information of the participants. The Royal Victorian Eye and Ear Hospital approved this study (ethics approval 16.1262H), and all participants provided written informed consent.

As part of a broader study, which encompassed both task-based experiments and resting-state recordings used in this study, we assessed the cognitive skills of our participants and evaluated the norm via age-normed percentiles before implantation. This assessment involved administering the trial-making tests A and B, as described by Tombaugh (2004). Test A required participants to draw lines between ascending numbers, while test B involved drawing lines between numbers and letters in ascending order alternatively. Participants were instructed to complete the tasks as quickly and accurately as possible without removing the pencil from the paper. It is important to note that all participants demonstrated normal performance and met the criteria for passing the tests.

This study aimed to introduce predictors for speech understanding outcomes of CI users after 1 year. Therefore, the speech understanding outcomes were measured at 12 months postimplant. Each participant underwent two audio-only speech tests to measure their speech understanding performance. Direct audio inputs were applied to remove the effect of any residual hearing on the speech perception measurements with the device. The first test included 50 consonant-nucleus-consonant (CNC) words in quiet (Peterson & Lehiste 1962). For this test, the overall scores were presented in percentages for both correct phonemes and words. The second test comprised 16 Bamford-Kowal-Bench (BKB) sentences in a multitalker bubble noise environment (Dawson et al. 2013). The test's score was determined based on the signal to noise ratio (SNR) needed to achieve 50% accuracy in word recognition. This SNR was adaptively adjusted during the test based on the participant's response accuracy. If the accuracy rate exceeded 50%, the SNR was reduced by 1 unit, while it was increased by 1 unit if the accuracy rate fell below 50%. This process was repeated 10 times, and the SNR values were averaged across the turning points of these iterations. Therefore, lower scores, indicating a lower SNR for achieving 50% word recognition, reflected better performance on the test. The SNR adjustment procedure for the BKB sentences began at 20 dB SNR. In both speech understanding tests, the speech was presented at a level of 65 dBA in the sound field, and the noise level was adapted to manipulate the SNR.

Data Acquisition

We recorded 5-minute resting-state fNIRS data at four time points, as previous studies have shown that this duration is sufficient to obtain reliable FC measurements using fNIRS (Birn et al. 2013; Geng et al. 2017; Aarabi & Huppert 2019). The first recording was before implantation; the rest were at 1, 3, and 12 months post-switch on. The measurements were carried out using the NIRscout system (manufactured by NIRx company). The system uses LEDs with dual near-infrared wavelengths of 760 and 850 nm. Our montage included 16 sources and 16 detectors mounted on a 10 to 20 system cap, which together built 54 channels, as shown in Figure 1. Among these, two channels were short (with a 5 mm distance between source and detector pairs), used in the preprocessing steps to eliminate systemic artifacts from the long channels (Chen et al. 2020). The mean distance between source and detectors of the long channels was 30 ± 6 mm. Data were sampled at a frequency of 7.8 Hz. Our regions of interest included bilateral temporal lobes and left prefrontal and occipital areas. (See Figure S1 in Supplemental Digital Content 1, http://links.lww.com/EANDH/B464, which depicts the positions of the sources and detectors in the international system, and Table S1 in Supplemental Digital Content 1, http://links.lww.com/EANDH/B464, which shows the Montreal Neurological Institute and Monte Carlo coordinates for sources and detectors.)

Data Preprocessing

We performed data preprocessing using the NIRS toolbox (Santosa et al. 2018). First, the raw recordings were converted to optical density. We evaluated the quality of channels using the scalp coupling index (SCI) (Pollonini et al. 2014). Channels with SCI lower than 0.5 were indicated as bad ones and removed from the recordings. If the number of bad channels in each recording exceeded 26, the recording was removed from further analysis. Then, we applied the temporal derivative distribution repair method on the remained channels to improve signal quality by removing motion artifacts (Fishburn et al. 2019). Afterward, the optical signals were converted to oxy- and de-oxyhemoglobin (HbO and HbR) based on the modified

TABLE 1. Demographic information of the participants

Participant	Gender	Age at Implant	Implant Ear	Duration of Deafness (yr)	Implant Ear PTA* (dBHL)	Ear With Hearing Loss
GPN001	M	36	L	2	N.R.	L
GPN002	F	75	R	10	100	L & R
GPN003	M	73	L	50	120	L & R
GPN004	F	57	R	20	112	L & R
GPN006	F	64	L	20	87	L & R
GPN007	M	70	L	5	82	L
GPN008	F	73	L	5	88	L & R
GPN009	F	54	R	1	57	L & R
GPN0010	M	78	R	20	92	L & R
GPN0011	M	87	R	12	107	L & R
GPN0012	M	37	L	0.5	78	L
GPN0013	F	78	L	18	70	L & R
GPN0015	M	19	L	0.25	105	L & R
GPN0016	M	73	L	20	114	L & R
GPN0017	M	65	L	0.6	83	L & R
GPN0018	M	60	R	12	62	L & R
GPN0020	F	22	L	0.75	90	L
GPN0021	F	75	L	4	98	L & R
GPN0022	F	49	L	46	100	L & R
GPN0023	F	42	L	2	95	L & R
GPN0024	M	55	R	13	103	L & R
GPN0026	M	28	L	1.25	120	L
GPN0027	F	66	L	20	120	L & R

**PTA of 0.5, 1, and 2 kHz hearing thresholds.*
PTA, pure-tone average.

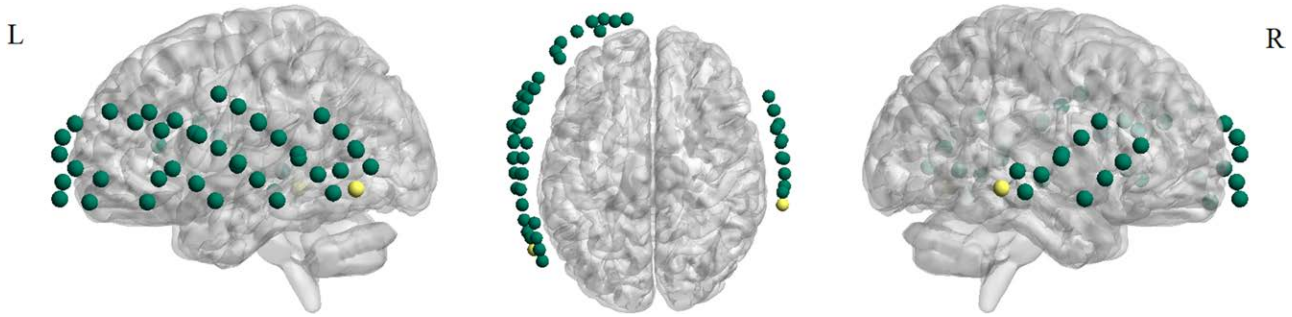

Fig. 1. The montage we used for resting-state fNIRS recording. It included 52 long channels (green) and 2 short channels (yellow). The montage covered bilateral temporal lobes and left prefrontal and occipital areas. fNIRS indicates functional near-infrared spectroscopy.

Beer-Lambert Law. As long channels capture both cerebral activities and systemic artifacts, such as heartbeats, respiration, and Myer waves, we took two successive steps to mitigate the effect of these systemic artifacts and other noises. We used short channels for short-channel correction and applied a band-pass filter with a 0.02 to 0.40 Hz passband. Short-channel correction regressed out short-channel signals that include systemic artifacts and no cerebral component (Santosa et al. 2020). The band-pass filter was applied to remove low-frequency artifacts like baseline drifts and high-frequency artifacts like heartbeats. In addition, using partial correlation to calculate correlations between pairs of channels helps eliminate common noise artifacts, such as Mayer waves, by regressing out shared components carried by other channels in the montage.

FC Matrix and Graph Construction

The connectivity analysis presented here is based on data in the HbO format. Previous studies have demonstrated that HbO produces more robust coherence patterns and connectivity compared with HbR (Wolf et al. 2011). However, we have also provided the main results based on HbR in the supplementary materials (see Figures and Tables in Supplemental Digital Content 2, http://links.lww.com/EANDH/B465, which include the HbR results). The average clustering coefficients in the brain networks and consequently, the results obtained from both hemodynamic chromophores are highly correlated (see Figure S2 in Supplemental Digital Content 2, http://links.lww.com/EANDH/B465). We measured FC between pairs of channels using regularized partial correlation. To illustrate constructing the functional brain network based on regularized partial correlation, suppose one performs multiple regression for each signal based on other signals as regressors. In that case, the regression slope for each regressor is proportional to the partial correlation coefficient between the signal and the regressor.

$$Y = X \cdot \beta + \varepsilon, \tag{1}$$

where X is an ($n \times p$) matrix and includes p controlling regressors with n samples each. β is a ($p \times 1$) vector of regression slopes for each controlling variable. ε is a vector of n elements showing the error terms in the linear estimations of the Y variable. The ordinary least squares method to solve the equation leads to the highest possible dimension for β that is p. However, partial correlation is usually calculated using regularization techniques. Regularization applies extra penalties for network complexity. Doing so removes partial correlation links between nodes (also known as edges in graph theory) that are likely to be spurious and help effectively to retrieve actual network structure (Epskamp & Fried 2018; Liégeois et al. 2020). This study used regularized partial correlation based on L2-norm Ridge Regression (aka Tikhonov) to estimate FC networks (Hoerl & Kennard 1970). The approach adds a term based on the squared sum of β values to the cost function:

$$f_{\text{cost}}(\beta, \lambda) = \sum_{i=1}^{n} \left(y_i - \sum_{j=1}^{p} x_{i,j}.\beta_j \right)^2 - \lambda \sum_{j=1}^{p} \beta_j^2 \tag{2}$$

λ parameter that ranges from 0 to 1 penalizes the β weights and control density in the FC graph to get rid of spurious links in the network. Higher values result in further shrinkage of the edge weights and sparser networks.

In this study, we used the leave-one-out cross-validation method to optimize λ for each speech understanding test (Kuhn & Johnson 2013). In this type of iterative method, one recording is left for testing each time, and others are used for training. The optimum λ value for each speech understanding test was chosen when the estimation error was minimum. Although leave-one-out is computationally expensive for large networks (e.g., in most fMRI studies), here, the cost was not a concern because our networks were relatively small (52 nodes).

Clustering Coefficient

In this study, we regarded the average clustering coefficients in the resting-state networks as features indicative of brain plasticity in CI users. We constructed signed weighted FC matrices based on partial correlation to measure connectivity between channels. Because correlation estimates for two signals are typically based on relatively short recordings, small amplitude correlations exist in the network as unstable estimates of correlations between nodes. Since these small amplitude partial coefficients are distributed equally between positive and negative weights, their effects are expected to be canceled out when averaging node clustering coefficients in the network. Therefore, compared with unsigned networks, in which absolute values of correlation are considered, signed networks demonstrate greater resistance to spurious connections (Costantini & Perugini 2014). In the FC networks (with weights from −1 to 1), the average clustering coefficient represented the overall connection density in the areas covered by the montage. We measured the clustering coefficient of node i in the signed weighted networks as,

$$\hat{C}_i = \frac{\sum_{j,q} \left(w_s(j,i)\, w_s(i,q)\, w_s(j,q) \right)}{\sum_{j \neq q} \left| w_s(j,i)\, w_s(i,q) \right|} \tag{3}$$

$w_s(i, q)$ is the edge weight connecting node a to node b. (i, j, q)s include all triangles with i as a vertex. The numerator is the sum of edge products of all triangles that include node i and the denominator equals the sum of absolute indirect traces between pairs of nodes that pass through node i (Rubinov & Sporns 2010; Costantini & Perugini 2014).

RESULTS

Construction of Brain Functional Networks Based on Regularized Partial Correlation

We calculated the resting-state FC networks of the fNIRS recordings using regularized partial correlation (Jenkinson et al. 2012). Figure 2 presents the effect of regularization on the FC matrix and weight distribution of a sample subject (subject seven, session three). As the figure shows, regularization has decreased the overall weight amplitudes and made the network sparser than the unregularized network by trying to remove spurious connections. Table 2 shows optimum regularization values (λ) for different tests across the sessions. The small (or zero) optimal λ values show that the regularization step had little (or no effect) on the complexity of networks in different sessions.

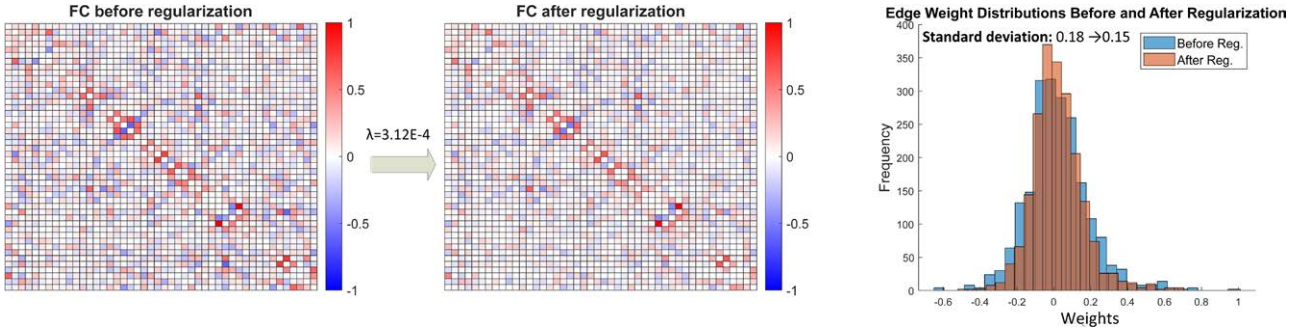

Fig. 2. Regularization effect on the FC weights for a sample subject (subject seven, session three). Regularization applies extra penalties on network complexity to eliminate spurious connections, resulting in weight distribution shrinkage. FC indicates functional connectivity.

Clustering Coefficient at Resting State Correlates With Speech Understanding Scores at 12 mo Postimplantation

We investigated the association between the average clustering coefficients in the signed weighted networks derived from the fourth recording session (at 12 mo) and the respective speech understanding outcomes of CI recipients after 1 year. Our analysis unveiled a statistically significant correlation between the average clustering coefficients and all categories of speech understanding scores at the 12-month assessment: including CNC words and phonemes in quiet, as well as BKB sentences in noise (Fig. 3).

To ensure the robustness of our findings, we generated 30 null networks for each FC network following the method described by (Rubinov & Sporns 2011). These null models were designed to serve as control graphs, maintaining connection weight distribution and node strength that closely resembled those of the primary networks. Figure 4 compares the p values of the correlation between speech scores and the average clustering coefficient for the primary and null graphs. The figure shows that the correlation between the average clustering coefficient and test scores for the null models reduced considerably (higher p values for null models).

TABLE 2. λ Values for each test across the sessions

	Speech Tests		
	CNC Quiet Words	CNC Quiet Phonemes	BKB Noise STR
Session 1	8.0E-6	8.0E-6	1.1E-4
Session 2	0	0	0
Session 3	0	0	0
Session 4	1.6E-4	2.8E-5	4.4E-4

BKB, Bamford-Kowal-Bench; CNC, consonant-nucleus-consonant; SRT, Speech reception threshold.

Average Clustering Coefficient in Resting-State Functional Networks Predict Implantation Outcomes

We extended our investigation to assess the correlation between the average clustering coefficients within the fNIRS resting-state networks recorded before implantation, as well as at 1 and 3 months postimplantation, and the corresponding speech scores obtained at the 12-month postimplantation assessment. These analyses provide valuable insights for practitioners, aiding in decision-making both before implantation and for adjusting the device postimplantation. Figure 5 summarizes the correlation values (R) between average clustering coefficients in the resting-state networks of each session with speech understanding scores. As the results indicated, in many cases, the average clustering coefficients of the brain networks at different time points before 1 year were highly correlated with behavioral CI outcomes at 12 months postimplantation.

Average Clustering Coefficient Reveals Brain Plasticity

Brain plasticity refers to the brain's remarkable ability to reorganize in response to sensory input. Following CI implantation, we anticipate the initiation of plastic changes spurred by the new stimuli provided by the device. To analyze these changes in the brain, we conducted an analysis to investigate

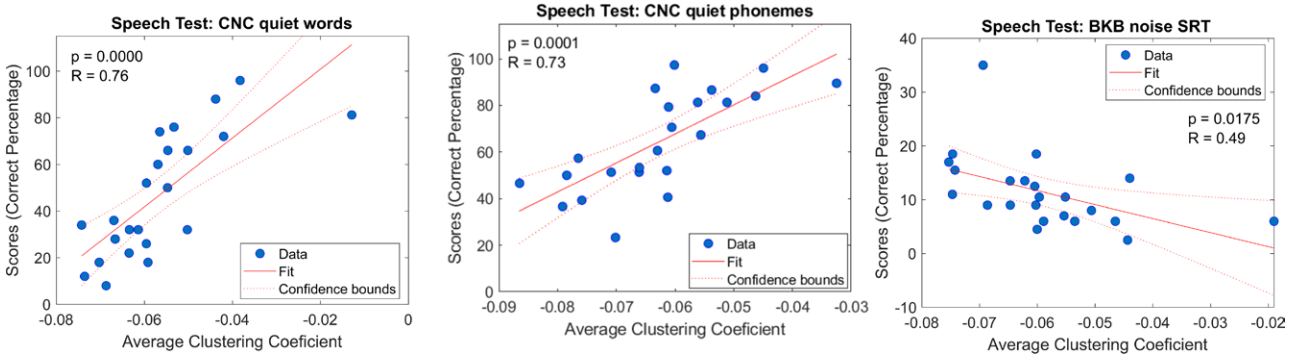

Fig. 3. Average clustering coefficient at 12 mo postimplantation correlates significantly with speech performance outcomes. BKB indicates Bamford-Kowal-Bench; CNC, consonant-nucleus-consonant; SRT, speech reception threshold.

alterations in the average clustering coefficient within the brain networks of our subjects across various sessions. As Figure 6 shows, the findings underscored a significant increase in the average clustering coefficients during the 3 and 12 months post-implantation when compared with the baseline values recorded preimplantation. However, no statistically significant changes were observed in the average clustering coefficient 1 month after the surgery.

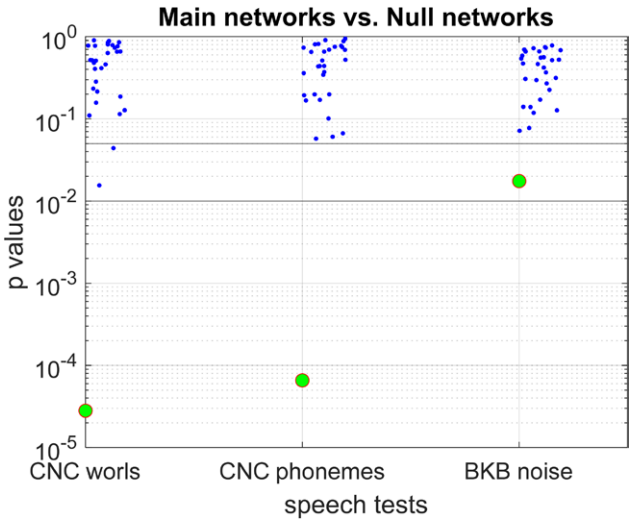

Fig. 4. Comparing the significance of the correlations between the speech scores and the average clustering coefficient in the primary (green circles) and null graphs (blue dots). The figure shows that the correlation dropped for null models considerably. BKB indicates Bamford-Kowal-Bench; CNC, consonant-nucleus-consonant.

Average Clustering Coefficient Convey Unique Information Beyond Age and Deafness Duration

Age and deafness duration are critical subject history factors known to impact cochlear implantation outcomes. Typically, older individuals and those with a longer duration of deafness tend to exhibit poorer speech outcomes. Notably, in our dataset, we compared the demographic profiles of subjects corresponding to the extreme data points in the correlation plots (with clustering coefficients smaller than −0.07 versus those with values greater than −0.05) of Figure 3 and found a significant difference in the mean age and deafness duration for these subjects. The average age and deafness duration for subjects with low average clustering, and consequently poorer speech performance, were 74 and 14.3 years, respectively, compared with 40 and 3 years for those with the highest average clustering coefficient and better speech performance.

As illustrated in Figure 7, the bar chart displays the correlation of these two factors (age and deafness duration) with speech scores. Notably, the correlation of age with speech scores, specifically CNC words and phonemes, is relatively high and comparable to the correlation between the average clustering coefficient and these scores. To comprehensively evaluate the individual contributions of these factors, we conducted multivariable linear regression analyses for each session. Before conducting these tests, we carefully examined multicollinearity among the variables. Detecting multicollinearity is crucial because, while it does not reduce the explanatory power of the model, it can diminish the statistical significance of the independent variables. To evaluate multicollinearity, we calculated the variance inflation factor (VIF), which measures the intercorrelation among independent variables in a multiple regression model (Daoud 2017). It is important to note that the VIF values for all variables in the multivariable regression

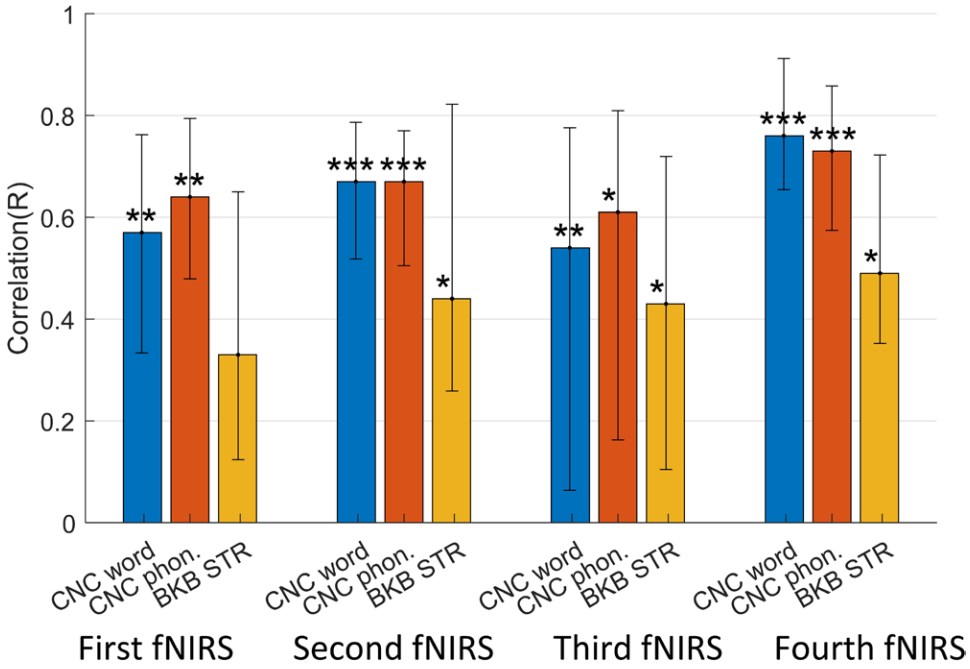

Fig. 5. Correlation (*R*) between speech scores and their predictions based on the linear regressors in each fNIRS recording session. The error bars show the 95% confidence interval for 100 bootstrapped samples. The star marks (*), (**), and (***) indicate *p* values smaller than the significance levels of $\alpha = 0.05$, 0.01, and $\alpha = 0.001$, respectively. BKB indicates Bamford-Kowal-Bench; CNC, consonant-nucleus-consonant; fNIRS, functional near-infrared spectroscopy; SRT, speech reception threshold.

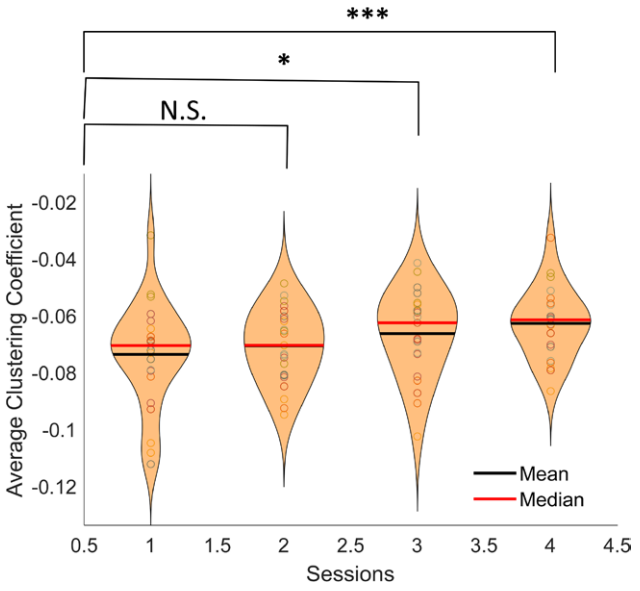

Fig. 6. The distribution of the average clustering coefficients of our subjects in different sessions. The changes in average clustering coefficients were significant at three and 12 mo but not in 1-mo postimplantation. *,*** indicate p values smaller than the significance levels of $\alpha = 0.05$ and $\alpha = 0.001$, respectively. N.S. indicates not significant.

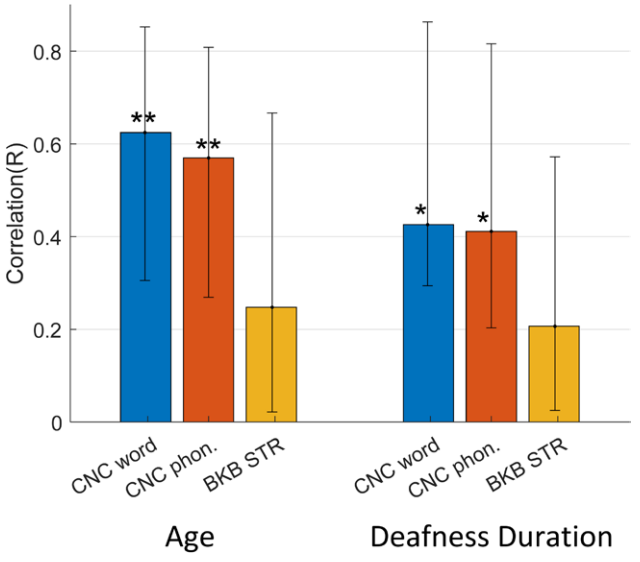

Fig. 7. The correlation between age and deafness duration with speech performance outcomes. *, ** indicate p values smaller than the significance levels of $\alpha = 0.05$ and $\alpha = 0.01$, respectively. BKB indicates Bamford-Kowal-Bench; CNC, consonant-nucleus-consonant; SRT, speech reception threshold.

tasks were below 2, with a maximum VIF of 1.86. These low VIF values indicate that multicollinearity is not a significant concern in our analysis.

Figure 8 presents a comparison of the correlation coefficients between age, deafness duration, and average clustering coefficient in four fNIRS recordings, considering them as independent variables, and speech understanding scores as dependent variables. The black squares in the bar plot denote the improvement in correlations compared with using only the average clustering coefficient as a predictive factor (Fig. 5).

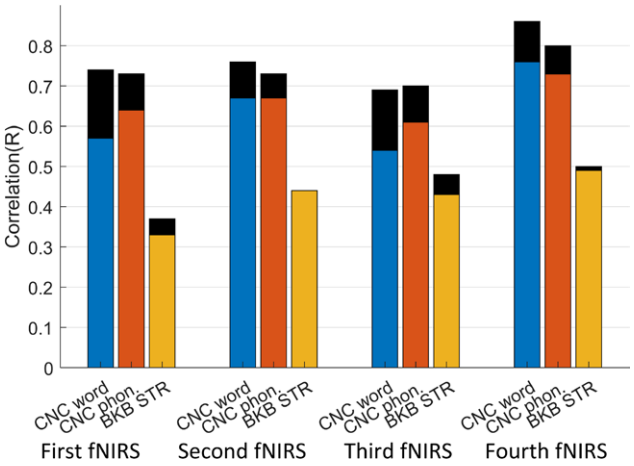

Fig. 8. Correlations between age, deafness duration, and average clustering coefficient in four fNIRS recordings as independent variables, and speech understanding scores as dependent variables. Black squares indicate enhanced correlations compared with using the average clustering coefficient alone as a predictive factor. BKB indicates Bamford-Kowal-Bench; CNC, consonant-nucleus-consonant; fNIRS, functional near-infrared spectroscopy; SRT, speech reception threshold.

Table 3 displays the p values from the F statistic test, indicating the significance level of a variable when considering the other terms in the model. Variables that remain significantly important in the model, even when accounting for other variables, are highlighted in bold in the table.

Channel Density Influences the Correlation Between Average Clustering Coefficient and Implantation Outcomes

In our study, the computation of partial correlation between channel pairs takes into account the influence of other channels within the montage. This consideration is vital as it can impact the resulting correlation values and, consequently, the average clustering coefficient, which we use as a predictive measure for patients' speech understanding performance following cochlear implantation. To delve deeper into this matter, we conducted experiments involving the removal of specific numbers of channels from the montage to assess the influence of channel density on our results. In each case, we randomly selected channels for removal from the setup and repeated this process 50 times for each number of omitted channels. Across different numbers of omitted channels, we calculated the average correlation between the average clustering coefficient and speech scores. Significantly, our results consistently indicate a trend: the reduction in channel density substantially decreased the accuracy of our proposed method across all sessions (refer to Fig. 9 for an example, illustrating our findings based on the second fNIRS recording session).

DISCUSSION

The objective of the present study was to evaluate resting-state cortical activity using fNIRS and to investigate a reliable indicator of cochlear implantation outcomes. Previous studies on FC often centered around task-based experiments. However, there has been a shift toward resting-state FC studies, primarily for investigating brain abnormalities, group differences, and providing diagnostic and prognostic biomarkers. This shift is

TABLE 3. Significance level of a variable considering other terms in the multiregression model

	First fNIRS			Second fNIRS			Third fNIRS			Fourth fNIRS		
	Score 1	Score 2	Score 3	Score 1	Score 2	Score 3	Score 1	Score 2	Score 3	Score 1	Score 2	Score 3
Clustering coefficient	0.127	**0.040**	0.290	**0.033**	**0.028**	**0.041**	0.181	**0.038**	0.091	**0.000**	**0.001**	**0.046**
Age	**0.015**	**0.041**	0.460	0.065	0.158	0.947	0.187	0.590	0.656	**0.038**	0.135	0.970
Deafness duration	0.796	0.994	0.910	0.557	0.580	0.955	0.203	0.136	0.399	0.085	0.300	0.587

Variables that remain significantly important in the model, even when accounting for other variables, are highlighted in bold.
fNIRS, functional near-infrared spectroscopy.

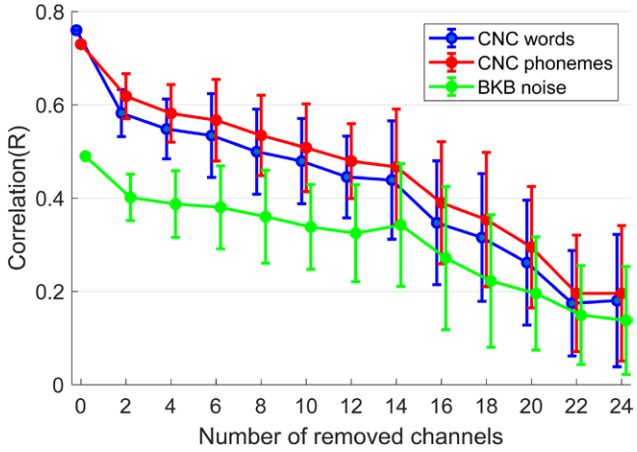

Fig. 9. Decreasing the channel density by randomly removing specific numbers of channels from the setup results in a reduced algorithm precision, as indicated by the correlation between the average clustering coefficient and different speech scores. We conducted 50 iterations for each number of removed channels for the fourth session. Error bars represent the variation introduced by removing different permutations of fNIRS channels. Error bars represent 1 SD from the mean. BKB indicates Bamford-Kowal-Bench; CNC, consonant-nucleus-consonant; fNIRS, functional near-infrared spectroscopy.

grounded in the fact that resting-state FC, also known as intrinsic brain FC, underpins task-based FC and operates across various brain states. Besides, the inconsistency in results from some task-based studies can be attributed to the diversity of tasks used in testing their hypotheses (Fullerton et al. 2023). Therefore, using resting-state recordings simplifies the study of brain networks by eliminating the need for numerous task scenarios (Fox & Greicius 2010; Cole et al. 2014). Accordingly, this study aimed to propose, for the first time in the literature, a simple and reliable biomarker for speech understanding performance of CI users based on resting-state brain FC.

In this study, we used partial correlation to measure FC between pairs of fNIRS signals and create signed weighted functional networks. Partial correlation is effective in removing spurious connections and mitigating the effects of systemic noise, which is a significant concern in many fNIRS studies. Studies have shown that the FC networks created by regularized partial correlation correlate better with the underlying structural neural network compared with other connectivity measures such as Pearson correlation (Liégeois et al. 2020). However, establishing the precise relationship between FC networks and structural networks, particularly for signed networks, is not straightforward, as most methods are developed for unsigned networks and do not consider the polarity of connections in the FC network (Damoiseaux & Greicius 2009; Messé et al. 2015; Liégeois et al. 2020).

The proposed measure in our study to interpret the variability in cochlear implantation outcomes was the average resting-state clustering coefficient in language brain areas covered by our montage, including bilateral temporal lobes and left prefrontal and occipital areas. We applied no restrictions in recruiting CI recipients, except that all participants were postlingually deaf and had been implanted with Nucleus brand devices. Despite the high variability among participants in terms of deafness duration, age, and the hearing condition of the other ear, our results demonstrated that this measure effectively explained

the variation in cochlear implantation outcomes and exhibited high reproducibility across pre- and postimplantation times. Consequently, it can offer specialists valuable insights before implantation to determine potential benefits for the patient, guide adjustments to the device after implantation, or prescribe rehabilitation strategies to improve hearing performance.

The clustering coefficient of a node in a graph indicates how well its neighbors are connected or correlated with each other in a functional network. Our results showed a positive correlation between the average clustering coefficient and speech outcomes, indicating that subjects with higher average clustering coefficients in the areas covered by the montage had better speech understanding performances. These regions of interest included bilateral temporal lobes and left prefrontal and occipital areas. Multiple studies have shown that hearing loss leads to brain atrophy in these brain areas involved in the language network, resulting in a reduction in neurons or neural connections (Yang et al. 2014; Jafari et al. 2021). The average clustering coefficient in the resting-state functional network can be interpreted as a measure of neural connection densities on a large scale because a high microscale correlation between resting-state functional and structural networks has been observed in many studies (Damoiseaux & Greicius 2009; Straathof et al. 2019). Our study has shown that patients with higher average clustering coefficients (presumably interpreted as less atrophy) perform better with the CI.

The average clustering coefficient at different time points revealed gradual plasticity in the FC network after the CI switch-on (Fig. 6). The results indicated that the average clustering coefficient increased after implantation due to the new stimuli provided by the device, aligning with the process of auditory recovery (Fallon et al. 2008; Strelnikov et al. 2015). Our findings showed that these changes were gradual and statistically significant after 3 months but insignificant for the first recordings taken 1 month after implantation. This pattern is in line with earlier research, which suggests that in the initial months following implantation, hearing remains suboptimal, and the sounds perceived are often challenging to decipher (Tyler et al. 1997).

We also conducted a comparative analysis to assess the predictive performance of the average clustering coefficient in resting-state networks in relation to subject-specific historical factors such as age and deafness duration concerning speech outcomes. Deafness duration, as reported by subjects, is inherently subjective, leading to varying interpretations among different individuals. Consequently, it emerges as a less reliable predictor, and its correlation with performance outcomes in our dataset was notably weaker compared with the correlation with age. Our findings reveal that the inclusion of our proposed measure alongside subject-specific factors substantially enhances the accuracy of outcome estimation across all time steps, as illustrated in Figure 8. Moreover, the results highlight that our proposed measure consistently accounts for variability in speech understanding outcomes not elucidated by recipient history factors. This is especially notable during the second recording, 1-month postimplantation, a crucial period for clinicians fine-tuning the device (Table 3). This highlights the unique information about brain plasticity conveyed by our measure, information not captured by age or deafness duration alone.

The present study focused on the auditory and specific parts of the left visual cortex, limiting the assessment of brain plasticity. Including interconnected regions like motor and broader visual areas would provide a more comprehensive evaluation, capturing adaptive and cross-modal changes. Another metric, brain modularity, could also be explored. Modularity, representing densely connected subnetworks with sparse connections in real-life networks, underpins brain segregation (Fornito et al. 2016; Friston & Buzsáki 2016). Studies suggest that sensory cortices, including hearing-related areas, experience atrophy and are influenced by remaining sensory areas like visual and motor regions (Bavelier & Neville 2002; Pavani & Röder 2012). With hearing loss, the auditory cortex's modularity may decrease due to reduced connections within the auditory module and enhanced connections with other areas, reflecting cross-modal plasticity. Postimplantation, the brain's capacity to regain modularity might correlate with enhanced device performance.

The arrangement of channels in the montage plays a pivotal role in partial correlation calculations and, consequently, influences the average clustering coefficient used for postimplantation speech understanding predictions. Our experiments, involving random channel removals, clearly demonstrated that decreased channel density resulted in diminished algorithm precision. This underscores the critical significance of channel density in algorithm performance and suggests avenues for future research to optimize channel density, potentially enhancing the measure's accuracy.

CONCLUSION AND FUTURE STUDIES

Our study aimed to identify an indicator elucidating adaptive brain changes post-hearing loss and cochlear implantation, illuminating variations in outcomes among postlingually deaf adults via fNIRS recordings. We used the average clustering coefficient within specific brain regions: bilateral temporal lobes and left prefrontal and occipital areas.

Consistent correlations between pre- and 1-year postimplantation clustering coefficients and speech understanding outcomes were observed. Notably, clustering coefficients increased within the initial three months postimplantation, suggesting brain plasticity and potential auditory recovery. It is important to note that our metric provided unique insights beyond conventional factors like age and deafness duration, enhancing prediction accuracy.

Future research could expand to include additional cortical regions and explore additional graph features to deepen our understanding of other aspects of brain plasticity, such as cross-modal plasticity.

Our study also underscored the importance of channel density in predicting CI outcomes, advocating for its central consideration in future investigations.

ACKNOWLEDGMENTS

This study was supported by a grant from the Passe and Williams Foundation to Colette M. McKay. T. P. was supported by a Junior Fellowship from the Passe and Williams Foundation. J. E. was supported by the University of Melbourne Research Scholarship. The Bionics Institute acknowledges the support it receives from the Victorian Government through its Operational Infrastructure Support Program.

C. M. M. designed the study and contributed toward data acquisition. J. E., T. P., B. J., and D. M. performed data analysis. All authors interpreted the data. J. E. drafted the manuscript. All authors critically reviewed the manuscript before submission.

The manuscript preprint is available at https://www.medrxiv.org/content/10.1101/2024.01.30.24301908v1.

The authors have no conflicts of interest to disclose.

Address for correspondence: Jamal Esmaelpoor, Department of Medical Bionics, University of Melbourne, 384 Albert Street, East Melbourne, VIC 3002, Australia. E-mail: jesmaelpoor@bionicsinstitute.org

Received December 20, 2023; accepted June 23, 2024

REFERENCES

Aarabi, A., & Huppert, T. J. (2019). Assessment of the effect of data length on the reliability of resting-state fNIRS connectivity measures and graph metrics. *Biomed Signal Proc Control*, *54*, 101612.

Anderson, C. A., Wiggins, I. M., Kitterick, P. T., Hartley, D. E. H. (2017). Adaptive benefit of cross-modal plasticity following cochlear implantation in deaf adults. *Proc Natl Acad Sci USA*, *114*, 10256–10261.

Bavelier, D., & Neville, H. J. (2002). Cross-modal plasticity: Where and how? *Nat Rev Neurosci*, *3*, 443–452.

Birn, R. M., Molloy, E. K., Patriat, R., Parker, T., Meier, T. B., Kirk, G. R., Nair, V. A., Meyerand, M. E., Prabhakaran, V. (2013). The effect of scan length on the reliability of resting-state fMRI connectivity estimates. *Neuroimage*, *83*, 550–558.

Blamey, P., Artieres, F., Başkent, D., Bergeron, F., Beynon, A., Burke, E., Dillier, N., Dowell, R., Fraysse, B., Gallego, S., Govaerts, P.J. (2012). Factors affecting auditory performance of postlinguistically deaf adults using cochlear implants: An update with 2251 patients. *Audiol Neurootol*, *18*, 36–47.

Boisvert, I., Reis, M., Au, A., Cowan, R., Dowell, R. C. (2020). Cochlear implantation outcomes in adults: A scoping review. *PLoS One*, *15*, e0232421.

Bullmore, E., & Sporns, O. (2012). The economy of brain network organization. *Nat Rev Neurosci*, *13*, 336–349.

Calvert, G. A., Bullmore, E. T., Brammer, M. J., Campbell, R., Williams, S. C. R., McGuire, P. K., Woodruff, P. W. R., Iversen, S. D., David, A. S. (1997). Activation of auditory cortex during silent lipreading. *Science*, *276*, 593–596.

Carlson, H. L., Craig, B. T., Hilderley, A. J., Hodge, J., Rajashekar, D., Mouches, P., Forkert, N. D., Kirton, A. (2020). Structural and functional connectivity of motor circuits after perinatal stroke: A machine learning study. *Neuroimage Clin*, *28*, 102508.

Cecchetti, G., Agosta, F., Basaia, S., Cividini, C., Cursi, M., Santangelo, R., Caso, F., Minicucci, F., Magnani, G., Filippi, M. (2021). Resting-state electroencephalographic biomarkers of Alzheimer's disease. *Neuroimage Clin*, *31*, 102711.

Chen, L. -C., Sandmann, P., Thorne, J. D., Bleichner, M. G., Debener, S. (2016). Cross-modal functional reorganization of visual and auditory cortex in adult cochlear implant users identified with fNIRS. *Neural Plast*, *2016*, 4382656.

Chen, W. -L., Wagner, J., Heugel, N., Sugar, J., Lee, Y. -W., Conant, L., Malloy, M., Heffernan, J., Quirk, B., Zinos, A., Beardsley, S. A., Prost, R., Whelan, H. T. (2020). Functional near-infrared spectroscopy and its clinical application in the field of neuroscience: Advances and future directions. *Front Neurosci*, *14*, 724.

Cole, M. W., Bassett, D. S., Power, J. D., Braver, T. S., Petersen, S. E. (2014). Intrinsic and task-evoked network architectures of the human brain. *Neuron*, *83*, 238–251.

Costantini, G., & Perugini, M. (2014). Generalization of clustering coefficients to signed correlation networks. *PLoS One*, *9*, e88669.

Craddock, R. C., Holtzheimer III, P. E., Hu, X. P., Mayberg, H. S. (2009). Disease state prediction from resting state functional connectivity. *Magn Reson Med e*, *62*, 1619–1628.

Damoiseaux, J. S., & Greicius, M. D. (2009). Greater than the sum of its parts: A review of studies combining structural connectivity and resting-state functional connectivity. *Brain Struct Funct*, *213*, 525–533.

Daoud, J. I. (2017). Multicollinearity and regression analysis. *J Phys Conf Ser*, *949*, 012009.

Dawson, P. W., Hersbach, A. A., Swanson, B. A. (2013). An adaptive Australian sentence test in noise (AuSTIN). *Ear Hear*, *34*, 592–600.

Doucet, M. E., Bergeron, F., Lassonde, M., Ferron, P., Lepore, F. (2006). Cross-modal reorganization and speech perception in cochlear implant users. *Brain*, *129*, 3376–3383.

Dunn, C. C., Walker, E. A., Oleson, J., Kenworthy, M., Van Voorst, T., Tomblin, J. B., Ji, H., Kirk, K. I., McMurray, B., Hanson, M., Gantz, B. J. (2014). Longitudinal speech perception and language performance in pediatric cochlear implant users: The effect of age at implantation. *Ear Hear*, *35*, 148–160.

Epskamp, S., & Fried, E. I. (2018). A tutorial on regularized partial correlation networks. *Psychol Methods*, *23*, 617–634.

Escrichs, A., Biarnes, C., Garre-Olmo, J., Fernández-Real, J. M., Ramos, R., Pamplona, R., Brugada, R., Serena, J., Ramió-Torrentà, L., Coll-De-Tuero, G., Gallart, L., Barretina, J., Vilanova, J. C., Mayneris-Perxachs, J., Essig, M., Figley, C. R., Pedraza, S., Puig, J., Deco, G. (2021). Whole-brain dynamics in aging: Disruptions in functional connectivity and the role of the rich club. *Cereb Cortex*, *31*, 2466–2481.

Fallon, J. B., Irvine, D. R. F., Shepherd, R. K. (2008). Cochlear implants and brain plasticity. *Hear Res*, *238*, 110–117.

Fishburn, F. A., Ludlum, R. S., Vaidya, C. J., Medvedev, A. V. (2019). Temporal derivative distribution repair (TDDR): A motion correction method for fNIRS. *Neuroimage*, *184*, 171–179.

Fornito, A., Zalesky, A., Bullmore, E. (2016). *Fundamentals of Brain Network Analysis*. Academic Press.

Fox, M. D., & Greicius, M. (2010). Clinical applications of resting state functional connectivity. *Front Syst Neurosci*, *4*, 1443.

Friston, K., & Buzsáki, G. (2016). The functional anatomy of time: What and when in the brain. *Trends Cogn Sci*, *20*, 500–511.

Fullerton, A. M., Vickers, D. A., Luke, R., Billing, A. N., McAlpine, D., Hernandez-Perez, H., Peelle, J. E., Monaghan, J. J. M., McMahon, C. M. (2023). Cross-modal functional connectivity supports speech understanding in cochlear implant users. *Cereb Cortex*, *33*, 3350–3371.

Geng, S., Liu, X., Biswal, B. B., Niu, H. (2017). Effect of resting-state fNIRS scanning duration on functional brain connectivity and graph theory metrics of brain network. *Front Neurosci*, *11*, 392.

Glennon, E., Svirsky, M. A., Froemke, R. C. (2020). Auditory cortical plasticity in cochlear implant users. *Curr Opin Neurobiol*, *60*, 108–114.

Gordon, K. A., Wong, D. D. E., Valero, J., Jewell, S. F., Yoo, P., Papsin, B. C. (2011). Use it or lose it? Lessons learned from the developing brains of children who are deaf and use cochlear implants to hear. *Brain Topogr*, *24*, 204–219.

Hoerl, A. E., & Kennard, R. W. (1970). Ridge regression: Biased estimation for nonorthogonal problems. *Technometrics*, *42*, 80–67.

Jafari, Z., Kolb, B. E., Mohajerani, M. H. (2021). Age-related hearing loss and cognitive decline: MRI and cellular evidence. *Ann N Y Acad Sci*, *1500*, 17–33.

Jenkinson, M., Beckmann, C. F., Behrens, T. E. J., Woolrich, M. W., Smith, S. M. (2012). Fsl. *Neuroimage*, *62*, 782–790.

Kim, E., Kang, H., Han, K. -H., Lee, H. -J., Suh, M. -W., Song, J. -J., Oh, S. -H. (2021). Reorganized brain white matter in early-and late-onset deafness with diffusion tensor imaging. *Ear Hear*, *42*, 223–234.

Kollndorfer, K., Fischmeister, F. P. S., Kowalczyk, K., Hoche, E., Mueller, C. A., Trattnig, S., Schöpf, V. (2015). Olfactory training induces changes in regional functional connectivity in patients with long-term smell loss. *Neuroimage Clin*, *9*, 401–410.

Kral, A., & Sharma, A. (2023). Crossmodal plasticity in hearing loss. *Trends Neurosci*, *46*, 377–393.

Kuhn, M., & Johnson, K. (2013). Applied Predictive Modeling *(Vol. 26)*. Springer.

Lazard, D. S., Vincent, C., Venail, F., de Heyning, P., Truy, E., Sterkers, O., Skarzynski, P. H., Skarzynski, H., Schauwers, K., O'Leary, S. (2012). Pre-, per-and postoperative factors affecting performance of postlinguistically deaf adults using cochlear implants: A new conceptual model over time. PLoS One, *7*, e48739.

Liang, C., Houston, L. M., Samy, R. N., Abedelrehim, L. M. I., Zhang, F. (2018). Cortical processing of frequency changes reflected by the acoustic change complex in adult cochlear implant users. *Audiol Neurootol*, *23*, 152–164.

Liégeois, R., Santos, A., Matta, V., Van De Ville, D., Sayed, A. H. (2020). Revisiting correlation-based functional connectivity and its relationship with structural connectivity. *Netw Neurosci*, *4*, 1235–1251.

Merabet, L. B., & Pascual-Leone, A. (2010). Neural reorganization following sensory loss: The opportunity of change. *Nat Rev Neurosci*, *11*, 44–52.

Messé, A., Rudrauf, D., Giron, A., Marrelec, G. (2015). Predicting functional connectivity from structural connectivity via computational models using MRI: An extensive comparison study. *Neuroimage*, *111*, 65–75.

Moore, D. R., & Shannon, R. V. (2009). Beyond cochlear implants: Awakening the deafened brain. *Nat Neurosci*, *12*, 686–691.

Pavani, F., & Röder, B. (2012). Crossmodal plasticity as a consequence of sensory loss: Insights from blindness and deafness. In Barry E. Stein

(Eds.), *The New Handbook of Multisensory Processes*, (pp. 737–759). The MIT Press.

Peelle, J. E. (2019). The neural basis for auditory and audiovisual speech perception. In William F. Katz, Peter F. Assmann (Eds.), *The Routledge Handbook of Phonetics* (pp. 193–216). Taylor & Francis.

Peterson, G. E., & Lehiste, I. (1962). Revised CNC lists for auditory tests. *J Speech Hear Disord*, *27*, 62–70.

Pollonini, L., Olds, C., Abaya, H., Bortfeld, H., Beauchamp, M. S., Oghalai, J. S. (2014). Auditory cortex activation to natural speech and simulated cochlear implant speech measured with functional near-infrared spectroscopy. *Hear Res*, *309*, 84–93.

Rubinov, M., & Sporns, O. (2010). Complex network measures of brain connectivity: Uses and interpretations. *Neuroimage*, *52*, 1059–1069.

Rubinov, M., & Sporns, O. (2011). Weight-conserving characterization of complex functional brain networks. *Neuroimage*, *56*, 2068–2079.

Sandmann, P., Dillier, N., Eichele, T., Meyer, M., Kegel, A., Pascual-Marqui, R. D., Marcar, V. L., Jäncke, L., Debener, S. (2012). Visual activation of auditory cortex reflects maladaptive plasticity in cochlear implant users. *Brain*, *135*, 555–568.

Santosa, H., Zhai, X., Fishburn, F., Huppert, T. (2018). The NIRS brain AnalyzIR toolbox. *Algorithms*, *11*, 73.

Santosa, H., Zhai, X., Fishburn, F., Sparto, P. J., Huppert, T. J. (2020). Quantitative comparison of correction techniques for removing systemic physiological signal in functional near-infrared spectroscopy studies. *Neurophotonics*, *7*, 35009.

Shader, M. J., Luke, R., Gouailhardou, N., McKay, C. M. (2021). The use of broad vs restricted regions of interest in functional near-infrared spectroscopy for measuring cortical activation to auditory-only and visual-only speech. *Hear Res*, *406*, 108256.

Straathof, M., Sinke, M. R. T., Dijkhuizen, R. M., Otte, W. M. (2019). A systematic review on the quantitative relationship between structural and functional network connectivity strength in mammalian brains. *J Cereb Blood Flow Metab*, *39*, 189–209.

Strelnikov, K., Marx, M., Lagleyre, S., Fraysse, B., Deguine, O., Barone, P. (2015). PET-imaging of brain plasticity after cochlear implantation. *Hear Res*, *322*, 180–187.

Strelnikov, K., Rouger, J., Demonet, J. -F., Lagleyre, S., Fraysse, B., Deguine, O., Barone, P. (2013). Visual activity predicts auditory recovery from deafness after adult cochlear implantation. *Brain*, *136*, 3682–3695.

Tombaugh, T. N. (2004). Trail Making Test A and B: Normative data stratified by age and education. *Arch Clin Neuropsychol*, *19*, 203–214.

Tyler, R. S., Parkinson, A. J., Woodworth, G. G., Lowder, M. W., Gantz, B. J. (1997). Performance over time of adult patients using the Ineraid or Nucleus cochlear implant. *J Acoust Soc Am*, *102*, 508–522.

Wolf, U., Toronov, V., Choi, J. H., Gupta, R., Michalos, A., Gratton, E., Wolf, M. (2011). Correlation of functional and resting state connectivity of cerebral oxy-, deoxy-, and total hemoglobin concentration changes measured by near-infrared spectrophotometry. *J Biomed Opt*, *16*, 087013.

Yang, M., Chen, H. -J., Liu, B., Huang, Z. -C., Feng, Y., Li, J., Chen, J. -Y., Zhang, L. -L., Ji, H., Feng, X., Zhu, X., Teng, G. -J. (2014). Brain structural and functional alterations in patients with unilateral hearing loss. *Hear Res*, *316*, 37–43.

Yu, Y., Meng, F., Zhang, L., Liu, X., Wu, Y., Chen, S., Tan, X., Li, X., Kuang, S., Sun, Y., Luo, B. (2021). A multi-domain prognostic model of disorder of consciousness using resting-state fMRI and laboratory parameters. *Brain Imaging Behav*, *15*, 1966–1976.